

# Day- and Night-time SLR at MHz Repetition Rate in Graz

Peiyuan Wang (1), Michael Steindorfer, Franz Koidl, Georg Kirchner

(1) Space Research Institute, Austrian Academy of Sciences, Austria  
([Peiyuan.Wang@oeaw.ac.at](mailto:Peiyuan.Wang@oeaw.ac.at))

## Abstract

Using ultra-high repetition rate lasers ( $\geq 100$  kHz) is one of the most promising strategies for the next generation of satellite laser ranging (SLR) systems. We present successful 1-MHz repetition rate SLR to laser cooperative targets up to inclined geosynchronous orbits at night-time. Among those, a maximum return rate of up to 53% was achieved, equivalent to 265 k returns per second for the satellite Swarm-B. In addition, day-time MHz SLR was realized by utilizing a propagated MHz range gate to reduce the massive background noise. Due to the high single shot resolution and massive data quantity, MHz SLR allows us to identify finer satellite signature effects in comparison to kHz systems. In future, MHz SLR will greatly improve current technology with respect to data amount and precision, shorter acquisition time, target signature detection or attitude determination.

## 1. Introduction

Within a global network of more than 40 stations, satellite laser ranging (SLR) measures the time of flight (ToF) with ultra-short pulses routinely between ground stations and satellites equipped with retro-reflectors (Pearlman et al., 2019). In the recent 20 years the kHz SLR technology has been practiced widely following the methods of SLR2000 (McGarry et al., 2004) and SLR Graz (Kirchner & Koidl, 2004). As a result of high repetition rate, ultra-short pulse width and low pulse energy, the performance of SLR has been significantly improved in terms of data density, accuracy, precision and stability, which enhances its unique contributions to the International Terrestrial Reference Frame (ITRF) (Altamimi et al., 2016). Consequently, it has become possible to distinguish individual retro-reflector cubes. This allows analyzing the spin rate, spin axis motion (Kucharski et al., 2009, 2012), signature (Kucharski et al., 2015) and attitude (Steindorfer et al., 2019) of satellites and space debris objects.

Currently no station within the International Laser Ranging Service (ILRS) operates routine SLR at ultra-high repetition rate ( $\geq 100$  kHz). In 2019 Matera SLR station has successfully tracked several satellites up to GNSS orbits at night-time using a 100 kHz, 9 ps pulse width, 100  $\mu$ J laser. Their results showed a single shot Root Mean Square (RMS) error of less than 50 ps and a normal point (NP) performance at mm level for most satellites. The GNSS data rate was increased by factor of 32 compared to their 10 Hz system. It allowed them to see the retro-reflector structure of satellites (Dequal et al., 2021). In another study of Stuttgart SLR station most challenges and benefits have been comprehensively discussed, such as the data precision and the burst mode operation (Hampf et al., 2019). Both works have revealed that ultra-high repetition rate SLR improves data quantity by at least one order of magnitude, which could provide datasets for higher accuracy orbit determination and increased resolution for spin and attitude analysis.

In this work we present the results of 1-MHz repetition rate SLR at Graz station, performed at night-time and also during daytime using propagated range gate calculation. The involved components, methods and setup are introduced. The achieved results should motivate SLR stations to upgrade their facilities and to conduct experiments with MHz lasers ultimately increasing the output and the accuracy of the whole ILRS network.

## 2. System Setup

The SLR system in Graz uses an altitude-azimuth mounted receive telescope with an integrated transmit telescope. The outgoing pulses of the MHz laser are guided through a first beam expander, a Coudé path and finally the transmit telescope, where the beam divergence can be adjusted dynamically for satellites at different altitudes to acquire an optimal return rate. A fast photodiode detects the leakage of a dielectric mirror and generates a 1-MHz signal to trigger the event timer (Artyukh et al., 2008). The incoming photons are collected by a receiving Cassegrain telescope with 50 cm diameter. Several additional cameras and detectors allow guidance during tracking, beam direction corrections and optoelectronic conversion. A silicon single-photon avalanche detector (SPAD) combined with a narrow spectral filter is used for the detection of the reflected laser photons from the satellite. The SPAD is equipped with a gating input which allows controlling the output of the detector only during the predicted arrival time of the reflected photons. The output of the SPAD is time-tagged by the same event timer as used for the laser start. The detailed specifications of the MHz SLR demonstration are given in Table 1.

**Table 1. The specifications of the MHz SLR setup**

MHz laser (neoMOS)	Wavelength	532 nm
	Energy per pulse	~7.8 $\mu$ J@1 MHz
	Repetition rate	up to 10 MHz
	Pulse width	< 10 ps
	Beam divergence at laser output	~1.75 mrad
Receiver	Aperture of the receive telescope	50 cm
	Bandwidth of the filter (FWHM)	3 nm@532 nm
SPAD (MPD)	Quantum efficiency	50%
	Dark count rate	< 100 counts/s
	Timing resolution jitter	less than 50 ps
	Dead time	typically 77 ns
	Sensitive area diameter	100 $\mu$ m

Above kHz repetition rate - even for low earth orbit (LEO) satellites – much more than one pulse travels simultaneously between ground and satellite. Therefore, controlling the triggering of the laser and the gating of the detector becomes a complex issue (Degnan, 1994). To avoid overlap between returning photons from the satellite and backscattered photons from the atmosphere, an additional delay of several tens of  $\mu$ s is introduced to the laser firing, if returned photons are expected at the same time. However, that is impracticable when the repetition rate of the SLR system is greater than 100 kHz, where the pulse interval is less than 10  $\mu$ s. Instead, a burst mode backscatter avoidance is used, at which the ranging scheme is scheduled into two phases (Fig. 1): During the transmitting phase, the laser is fired at its nominal repetition rate until 100

$\mu\text{s}$  before the predicted arrival time of the first reflected photon. After this transmitting phase the laser is turned off and a backscatter avoidance phase is started, waiting for the backscatter of the last sent laser pulse to arrive back at the station. The backscatter which might cause the overlap is assumed to come from a maximum range of about 15 km from the atmosphere, corresponding to  $\sim 100 \mu\text{s}$  2-way ToF. At the following receiving phase the detector is activated for another ToF -  $100 \mu\text{s}$  duration to collect all reflected photons. During that phase the laser remains switched off. This pattern is repeated and the period of the burst mode is tuned in real time according to the slant range of the satellite.

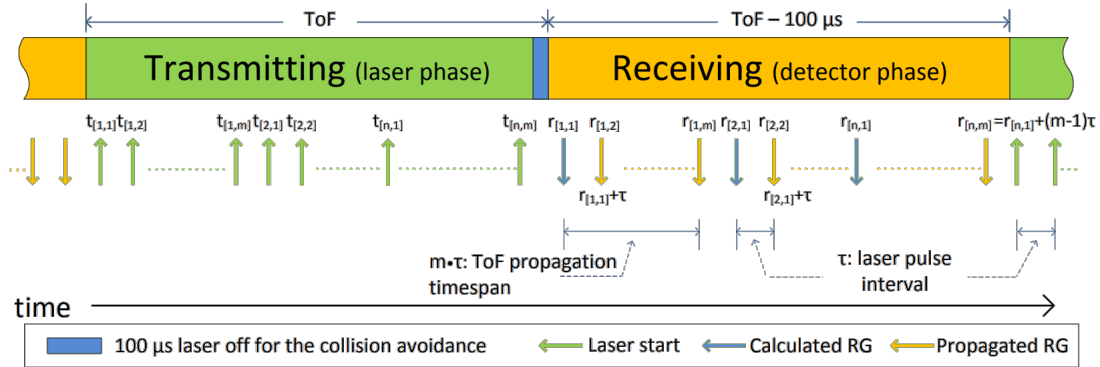


Fig. 1 MHz SLR timing sequences and the propagation method for RGG

At night-time the detector is continuously gated during each receiving phase (free running mode). However, the background noise during daytime is much higher than during nighttime. Therefore temporal (range gate), spatial (field of view of the receive optics) and ultra-narrow spectral filters are required to achieve an acceptable signal-to-noise ratio. In kHz SLR systems the range gate generator (RGG) is determined by each laser start epoch and the corresponding arrival time. According to these the detector is activated (gated) accordingly. For MHz SLR systems it is not possible to calculate range gates for each laser pulse due to the limit of CPU and hardware speed and the capacity of First-In First-Out (FIFO) memory within our Field Programmable Gate Array (FPGA).

The control timing of the RGG includes the measurement of the laser start epochs and the ToF calculation. It was found that within 100 ms the time intervals of MHz laser pulses vary within a maximum of peak-to-peak 1.2 ns. Without losing accuracy the ToF can be calculated periodically at fixed intervals  $m \cdot \tau$ , where  $m$  is a predefined value (200) and  $\tau$  is the time interval of 1-MHz pulses (approx.  $1 \mu\text{s}$ ). A propagated method for MHz RGG is illustrated in Fig. 1. The receiving phase is split into  $n$  fixed intervals each corresponding to  $m \cdot \tau = 200 \mu\text{s}$ . At the beginning of each interval a new range gate epoch  $r_{[n,1]} = t_{[n,1]} + \text{ToF}$  is calculated, where  $t_{[n,1]}$  is the measured start epoch of the corresponding laser pulse. For the following  $200 \mu\text{s}$  the range gate epochs are “propagated” according to  $r_{[n,m]} = r_{[n,1]} + (m-1) \cdot \tau$  using a delay circuit in the FPGA, until a new updated is calculated. At each propagated range gate, the detector is activated 100 ns before the expected returns and deactivated 100 ns after.

The method of the propagated RGG relies on the low peak-peak jitters of the laser pulse intervals and on periodically updating the ToF, keeping sufficient accuracy. This approximation is validated by calculating the deviation from the true ToF as compared a LEO satellite throughout the pass. The “worst case scenario” of a LEO satellite was chosen as for low elevations the change rate of the range (or the time derivative of the

ToF) is the largest where the deviation is the largest. For a pass of Swarm-B it was found that for intervals of the fixed ToF below 200  $\mu\text{s}$  the offset to the true ToF remains below 10 ns. This adds only up to a few ns to the inaccuracy of the RGG, but this is fully acceptable for daytime SLR.

This is worth mentioning that the detector used for this MHz has a self control circuit and it becomes active immediately after each avalanche (see table 1). The RG applied for daytime ranging only blocks the output signals of the detector. This provides an acceptance interval compensating the jittering of the laser start epoch, the periodical error of the calculation of the ToF, and the potential inaccuracy of the predictions during searching phase. Once returns are identified the range gate width is reduced to filter out more noise events. All detected receive event times within each range gate are stored and multiple returns can then be analyzed via post processing.

This propagated RGG method significantly reduces the workload for the FPGA regarding ToF calculation and memory demand by a factor of up to of  $m=200$  as compared to the traditional kHz method. It makes MHz SLR and post-processing practicable during day-time even against massive background noise.

The ranging PC software was developed for SP-DART(Kirchner et al., 2015) which has all features of a full SLR station. A few adaptations were introduced regarding multi-threading to process different tasks simultaneously. Furthermore, a down-sampling method was introduced to be able to display real-time range residuals at increased efficiency (selecting 1 out of 100 points for display).

### 3. Results

During the demonstration several ILRS satellites in different orbital heights were measured from LEO of few hundreds of km to inclined Geosynchronous Orbit (IGSO) orbit with more than 38,000 km. With a single pulse energy of only  $\sim 7.8 \mu\text{J}$  the maximum return rate reached more than 50% for LEO satellites (Swarm-B in Fig.2),  $\sim 1.0\%$  for HEO satellites (Galileo), and  $\sim 0.16\%$  for the geostationary orbit satellite (Beidou IGSO 5 in Fig.3) at night-time. With the help of the propagated MHz RGG, a number of day-time passes of LEO satellites were detected successfully (Fig. 4) during the very last few days of the demonstration.

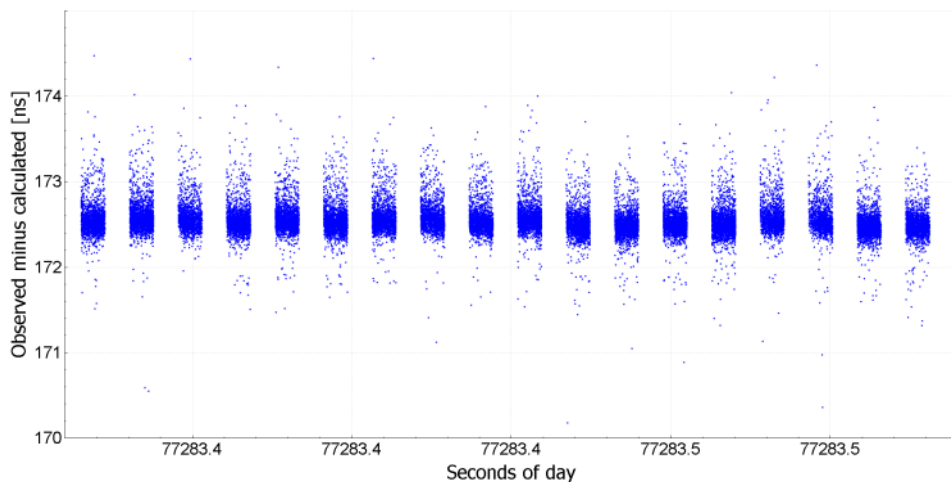


Fig.2 1-MHz Observed minus calculated residuals at night for Swarm-B (NORAD: 39451, with a slant range of  $\sim 570.0$  km and elevation angle of  $\sim 61.3^\circ$ ). Burst mode:

~3.8 ms duration for each transmitting and receiving phase. A maximum return rate of 53.0% was achieved, equivalent to ~265,150 returns per second (after iterative  $\pm 2.5$  sigma clipping).

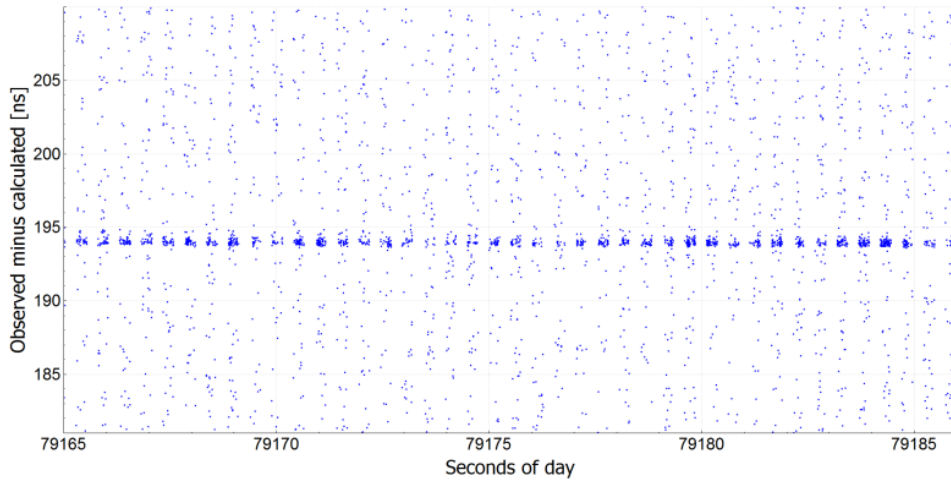


Fig.3 1-MHz observed minus calculated residuals at night for Beidou IGSO 5 (NORAD: 37948, with a slant range greater than 38,000 km and elevation angle of  $\sim 36.8^\circ$ ). Burst mode: ~255.4 ms duration for each transmitting and receiving phase. A maximum return rate of 0.16% was achieved, equivalent to ~800 returns per second (after iterative  $\pm 2.5$  sigma clipping).

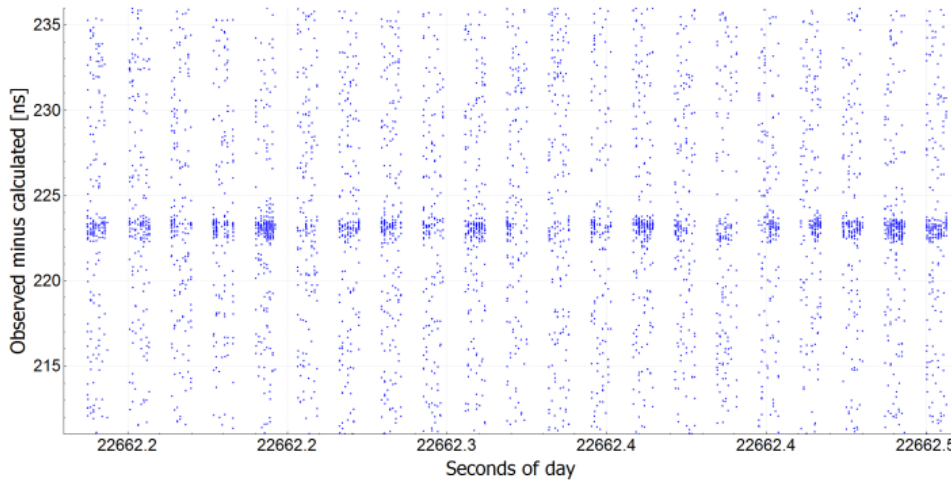


Fig.4 1-MHz daytime observed minus calculated residuals for Starlette (NORAD ID: 7646, with slant range of ~977.3 km and elevation angle of  $\sim 36.8^\circ$ ) at 06:17 UTC on July 19, 2020, the solar elevation angle greater than  $27^\circ$ . A maximum return rate of 2.15% was achieved, equivalent to 10,750 returns per second (after iterative  $\pm 2.5$  sigma clipping).

Compared to the conventional 2 kHz SLR system in Graz, the MHz SLR system leads to significantly higher return rates for LEO, HEO and IGSO (Fig. 5). According to the ILRS NP algorithm (*ILRS Normal Point Algorithm*), this will significantly improve the precision of the final NP results in view of statistical errors.

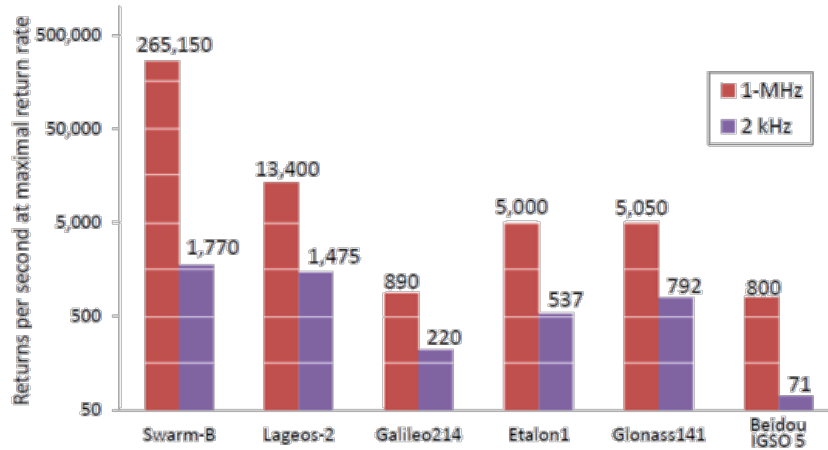


Fig.5 A comparison of returns per second between Graz 2 kHz system and 1-MHz demonstration in different orbits from LEO to IGSO. It exposes that a 1-MHz system contributes at least two magnitudes for some LEO satellites, and about one magnitude more data for high orbiters.

#### 4. Conclusion and Discussion

We present the design and the setup of SLR system at ultra-high repetition rate. We demonstrate the burst mode and a new concept of a propagated MHz RGG, and present results at day- and night-time at 1-MHz repetition rate. It has been successfully proven that such low pulse energies – and the corresponding low signal-to-noise relation - can be handled, despite the massive background noise during daytime. The number of returns per second has been increased significantly, as compared to our 2 kHz system.

Since kHz SLR (high data rate and low single shot RMS, single photon sensitivity) was introduced to ILRS it became possible to identify individual retro-reflectors in range residuals. Lots of studies and applications, taking benefits of the single shot RMS and the high density of measurements, have been made to analysis target spin rates and spin axis orientation. The detectability efficiency of MHz with the laser of some  $\mu\text{J}$  per pulse only is most time within single-photon regime. In our demonstration signature effects were clearly visible for most spherical and pyramidal CCR arrangements, such as Ajisai, Beacon-C, Envisat, Lageos, etc. MHz SLR deliveries a significantly higher data rate in comparison to kHz, which brings a finer tool in view of time resolution for this application. Fig. 6 illustrates ranging residuals of MHz measurements of Lares-2. Lares-2 is equipped with 303 pieces of one inch in diameter retro-reflectors, which are smaller than most geodetic satellites in order to minimize the signature effects (*LARES-2 (Laser Relativity Satellite-2)*, 2022). However, as the relative position and orientation vary between the satellite and Graz station, during the pass individual retro-reflector became ‘visible’ and ‘disappear’ alternately, while this can’t be seen in kHz measurements.

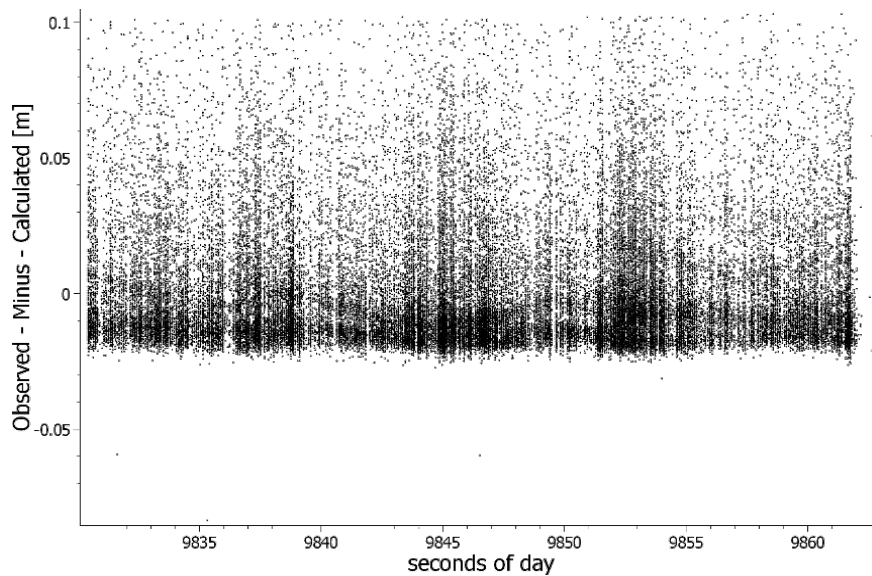


Fig. 6 Lares-2 residuals present individual retro-reflectors

In our opinion, in the near future MHz laser ranging might be a key concept for geodetic researches. It will further improve the precision of SLR measurements and can help acquiring more satellite passes and more Normal Points during each laser ranging session. In addition, it delivers higher time resolution to determine the spin rate and attitude motion of space targets.

The laser applied for this demonstration has a very compact dimension (554 \* 220 \* 90 mm<sup>3</sup>), that potentially delivers an opportunity for mounting it as a piggyback device on the telescope like demonstrated already in some stations (Kloth et al., 2018; Steindorfer et al., 2020), avoiding the long Coudé path and its regularly alignment.

Space debris laser ranging (SDLR) is an evolving application emerging from SLR. Diffuse reflections from uncooperative space debris targets (i.e. without retro-reflector) are detected while using powerful laser pulses (a few ns pulse width and > 10 Watt) (Greene et al., 2002; Kirchner et al., 2013; Liang et al., 2019). Although the lower pulse energy will decrease the detection probability (Degnan, 1993), this can be compensated by increasing the laser repetition rate. Poor prediction quality for non-cooperative targets will cause an ambiguity problem for such high repetition rates, but this can be fixed by slightly tuning repetition rate during tracking.

## References

Altamimi, Z., Rebischung, P., Métivier, L., & Collilieux, X., ITRF2014: A new release of the International Terrestrial Reference Frame modeling nonlinear station motions. *Journal of Geophysical Research: Solid Earth*, 121(8), 6109–6131. <https://doi.org/10.1002/2016JB013098>, 2016.

Artyukh, Y., Bepalko, V., Boole, E., & Vedin, V., Advances of High-precision Riga Event Timers. *Proceedings of the 16th International Workshop on Laser Ranging*, 398–403, 2008.

Degnan, J. J., Millimeter accuracy satellite laser ranging: A review. In *Contributions of*

*Space Geodesy to Geodynamics: Technology* (pp. 133–162). <https://doi.org/10.1029/GD025p0133>, 1993.

Degnan, J. J., SLR 2000: an automated, eyesafe satellite ranging station for the future. In Intergovernmental Panel on Climate Change (Ed.), *Proceedings of the 9th international workshop on laser ranging* (Vol. 53, Issue 9, p. 312). Australian Government Publishing Service, 1994. <https://doi.org/10.1017/CBO9781107415324.004>

Dequal, D., Agnesi, C., Sarrocco, D., Calderaro, L., Santamaria Amato, L., Sicilia de Cumis, M., Vallone, G., Villorosi, P., Luceri, V., & Bianco, G., 100 kHz satellite laser ranging demonstration at Matera Laser Ranging Observatory. *Journal of Geodesy*, 95(2), 26, 2021. <https://doi.org/10.1007/s00190-020-01469-2>

Greene, B., Gao, Y., & Moore, C., Laser Tracking of Space Debris. *13th International on Laser Ranging Workshop*, 1–7, 2002.

Hampf, D., Schafer, E., Sproll, F., Otsubo, T., Wagner, P., & Riede, W., Satellite laser ranging at 100 kHz pulse repetition rate. *CEAS Space Journal*, 11(4), 363–370, 2019. <https://doi.org/10.1007/s12567-019-00247-x>

*ILRS Normal Point Algorithm*. Retrieved December 31, 2022, from [https://ilrs.gsfc.nasa.gov/data\\_and\\_products/data/npt/npt\\_algorithm.html](https://ilrs.gsfc.nasa.gov/data_and_products/data/npt/npt_algorithm.html)

Kirchner, G., & Koidl, F., Graz kHz SLR system: design, experiences and results. *Proceedings of the 14th International Laser Ranging Workshop*, 53(9), 1689–1699, 2004. <https://doi.org/10.1017/CBO9781107415324.004>

Kirchner, G., Koidl, F., Friederich, F., Buske, I., Völker, U., & Riede, W., Laser measurements to space debris from Graz SLR station. *Advances in Space Research*, 51(1), 21–24, 2013. <https://doi.org/10.1016/j.asr.2012.08.009>

Kirchner, G., Steindorfer, M. A., Koidl, F., & Wang, P., SP-DART: Single-Photon Detection, Alignment and Reference Tool. *Proceedings of the ILRS Technical Workshop 2015*, 1, 1–7, 2015. [http://cddis.gsfc.nasa.gov/2015\\_Technical\\_Workshop/docs/papers/3.8\\_Kirchner\\_paper.pdf](http://cddis.gsfc.nasa.gov/2015_Technical_Workshop/docs/papers/3.8_Kirchner_paper.pdf)

Kloth, A., Steinborn, J., Munder, J., Zayer, I., Kirchner, G., Salmins, K., & Schildknecht, T., Towards Turnkey SLR Systems : New ESA Laser Ranging Station (ELRS). *Proceedings of the 21th International Workshop on Laser Ranging, 2018*.

Kucharski, D., Kirchner, G., Koidl, F., & Cristea, E., 10 Years of LAGEOS-1 and 15 years of LAGEOS-2 spin period determination from SLR data. *Advances in Space Research*, 43(12), 1926–1930, 2009. <https://doi.org/10.1016/j.asr.2009.01.019>

Kucharski, D., Kirchner, G., Otsubo, T., & Koidl, F., A method to calculate zero-signature satellite laser ranging normal points for millimeter geodesy - a case study with Ajisai. *Earth, Planets and Space*, 67(1), 34, 2015. <https://doi.org/10.1186/s40623-015-0204-4>

Kucharski, D., Otsubo, T., Kirchner, G., & Bianco, G., Spin rate and spin axis orientation of LARES spectrally determined from Satellite Laser Ranging data. *Advances in Space Research*, 50(11), 1473–1477, 2012. <https://doi.org/10.1016/j.asr.2012.07.018>

*LARES-2 (Laser Relativity Satellite-2)*, 2022. <https://www.eoportal.org/satellite-missions/lares-2#launch>

Liang, Z., Dong, X., Ibrahim, M., Song, Q., Han, X., Liu, C., Zhang, H., & Zhao, G., Tracking the space debris from the Changchun Observatory. *Astrophysics and Space Science*, 364(11), 201, 2019. <https://doi.org/10.1007/s10509-019-3686-x>

McGarry, J., Zagwodzki, T., Degnan, J., Cheek, J., Dunn, P., Mallama, T., Donovan, B., Patterson, D., & Mann, T., Early Satellite Tracking Results from SLR2000. *Proceedings of the 14th International Workshop on Laser Ranging, June, 1–6, 2004.*

Pearlman M.R., Noll C.E., Pavlis E.C., Lemoine F.G., Combrink L., Degnan J.D., Kirchner G., Schreiber U., The ILRS: approaching 20 years and planning for the future, *J. Geodesy*, 93, 2161-2180, 2019. DOI:10.1007/s00190-019-01241-1

Steindorfer, M. A., Kirchner, G., Koidl, F., Wang, P., Jilete, B., & Flohrer, T., Daylight space debris laser ranging. *Nature Communications*, 11(1), 3735, 2020. <https://doi.org/10.1038/s41467-020-17332-z>

Steindorfer, M. A., Kirchner, G., Koidl, F., Wang, P., Wirnsberger, H., Schoenemann, E., & Gonzalez, F., Attitude determination of Galileo satellites using high-resolution kHz SLR. *Journal of Geodesy*, 2019. <https://doi.org/10.1007/s00190-019-01284-4>